DYNAMIC DIGITAL IMAGE CORRELATION OF A DYNAMIC PHYSICAL MODEL OF THE VOCAL FOLDS

S. Mantha, L. Mongeau, T. Siegmund
School of Mechanical Engineering, Purdue University, IN, U.S.A.

Abstract: **An experimental study of the vibratory deformation of the human vocal folds was conducted. Experiments were performed using model vocal folds made of soft silicone rubber, and an air supply system. The model self-oscillated at fundamental frequencies and flow rates typical of the human folds. Time-averaged mass flow rates and transglottal pressures were measured along with the sound pressure upstream of the orifice. The deformation of the vocal fold was measured using a high-speed three-dimensional digital correlation system. The imaging set-up is composed of a high-speed digital camera and a prism beam splitter allowing two images to be obtained from different viewpoints in every image frame. Commercially available digital image correlation software was used to analyze the images, and to calculate the strain fields at the vocal fold superior surface. Results were obtained for vocal folds made of isotropic material and two different vocal fold lengths. The deformed shape of the model vocal folds, strains on the superior surface, and the time-varying vocal fold wall displacement were obtained.**

Keywords: Digital image correlation (DIC), high-speed video, strain fields, collision

I. INTRODUCTION

Many techniques are available for the visualization of laryngeal pathology. Methods based on inverse filtering of radiated voice sound pressure signals, for example, or electroglottography provide useful information about the mean flow rate and waveform of the glottal source. Optical techniques for the study of vocal fold vibrations have become readily available following the widespread use of high-speed digital photography. Among these optical methods, videoendoscopy, stroboscopy and high-speed photography have shown to provide a good visual impression of the vocal fold dynamics [1]. In addition kymographic image sequences allow for a convenient visualization of vibration patterns [2]. These widely known methods, however, provide little quantitative insight into the fundamental deformation processes taking place in the tissue during self-oscillation of the vocal folds. To obtain quantitative measures of deformation, a micro-suture technique was applied to study mucosal wave propagation [3]. This method is invasive and allows for measurement of only a few discrete image points. Another non-invasive method, laser triangulation, was used but this approach is again limited to only local measurement points [4].

In the present paper, the application of a digital image correlation (DIC) technique to the study of vocal fold dynamics and deformation is described. This method allows for noninvasive synchronous measurements of the entire displacement field of the deformed vocal folds. The capabilities of the technique were investigated using a physical model of the vocal fold system [5]. The results so far are encouraging, and suggest that the procedure can be successfully used provided a suitable speckle pattern can be applied onto the surface of the deformable body.

II. THE VOCAL FOLD MODEL

The physical models of the vocal folds were built for a generic vocal shape [5, 6] following procedures described in [7]. The material used to cast the model folds was a silicone rubber, Ecoflex, manufactured by [8]. The vocal folds were made of one single isotropic material. The material was characterized by a hardness value of H_{ooo}=31 on an OOO durometer scale. Uniaxial tensile tests were conducted. The tangent modulus at $\varepsilon = 0$ was determined to be E=5 Kpa. The magnitude of the elastic modulus is thus approximately within the lower range of the longitudinal elastic properties of the human vocal fold cover [9].

III. EXPERIMENTAL SET-UP

The experimental set-up used in the investigation is depicted in Figure 1. The main components included an air-supply system connected to an air duct assembly. The model larynx was assembled in a rigid frame with zero glottal opening. The frame containing the model larynx was placed at the upstream exit of the air duct. The experimental set-up was connected to a mass flow meter, a pressure transducer and a HP DAC system. Images of the superior surface of the model larynx were obtained by the use of a high-speed digital camera, Memrecam fx K3, NAC Image Technology, [10], at a frame rate of 3000 frames per second.

Models and analysis of vocal emissions for biomedical applications. 4th international workshop. October 29-31, 2005 – Firenze, Italy.
Edited by C. Manfredi. ISBN 88-8453-320-1 (online)

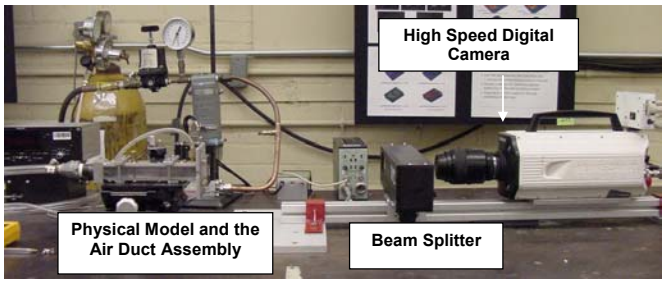

Figure 1: Experimental set-up.

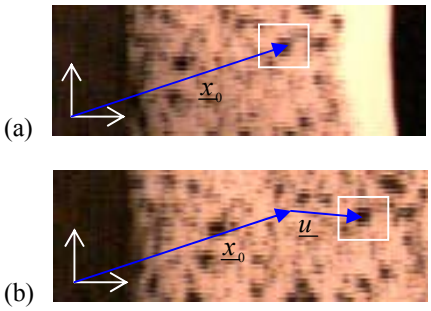

Figure 2: Tracking a point on the superior vocal fold surface from (a) a reference to (b) a deformed state through gray value patterns in subsets.

A 3D-DIC system was employed. The analysis consists of two steps: (a) a stereo correlation technique to determine in plane displacements (u, v) [11] and (b) stereo triangulation [12] to obtain the out-of-plane deformation (w). For the determination of the in-plane displacements through a DIC analysis, images of the object under consideration at two different stages of deformation were compared; see Fig. 2(a) for the image of the reference state and Fig. 2(b) for the image of the deformed state. The stereo correlation analysis requires that any point in the undeformed stage of the object, $\underline{x}_0$ is matched with the corresponding point in the deformed stage, $\underline{x} = \underline{x}_0 + \underline{u}$. In DIC, such a correlation is obtained by searching for matching gray scale patterns in corresponding images. So-called "subsets", i.e. parts of digital images, are traced via their gray value distribution from the undeformed reference image to the deformed image, as shown Fig. 2. The uniqueness of the matching lies on the creation of a non-repetitive speckle pattern on the object's surface. To obtain the speckle pattern, first a white pigment was mixed into the silicone rubber material during model preparation. Subsequently, black enamel paint was used to obtain the speckle pattern on the superior surface of the pseudo vocal folds. The application of the speckle pattern to the pseudo vocal folds is non-invasive and did not add any significant mass to the system.

For the stereo triangulation, two images of the object at each stage of deformation are required in order to obtain the out-of-plane displacement information. This was accomplished by obtaining two images of the object simultaneously in one single CCD frame at each time instant through the placement of a beam splitter in the optical axis between the camera and the model larynx, Fig. 3. With this set-up two images of the model larynx are obtained at offset image positions and are recorded on a common digital image frame. These images provide a "left" and "right" view of the model larynx. Thus, the deformed shape of the vocal folds can be obtained by triangulation.

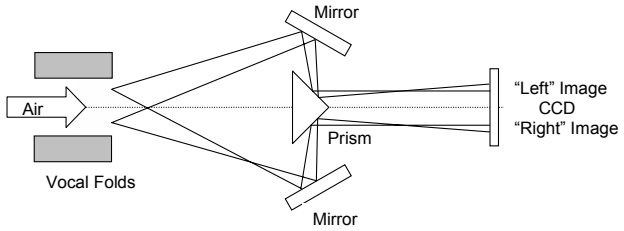

Figure 3: Image set-up with beam splitter. (Figure not to scale)

The digital image correlation analysis was performed using the program VIC-3D [13]. In the specific version of the program employed here, the image correlation was accomplished using an iterative spatial domain-correlation algorithm [14]. Calibration for focal length, image center and lens distortion was performed using a calibration target.

IV. RESULTS

Experiments were conducted on two larynx models with lengths $L = 17$ mm and 22 mm, respectively. First, for each model, the airflow rate was increased stepwise until self-oscillation was detected. Table 1 summarizes the phonation onset data. Phonation frequencies and onset pressures were within the range of physiological values. Six measurements were undertaken at higher mass flow rates, beyond the phonation threshold. The phonation frequency changed slightly as the mass flow rate was increased, Fig. 4(a). A maximum in the measured phonation frequency was reached for a flow rate of 550 cc/s. As discussed in the following, this behavior is associated with the onset of the occurrence of vocal fold closure and collision. Collision occurred at a vocal fold length dependent critical mass flow rate. For both models a linear relationship between pressure and mass flow rate was obtained, Fig. 4(b).

Kymographic images, shown in Figure 5, were obtained for L=22 mm at flow rates of 406 and 690 cm^3/s. These images clearly demonstrate the difference between the vibration processes at low and high flow rates. At low flow rates, no closing or collision of the vocal folds was observed. At larger flow rates, significant closure and collision takes place. Low and high flow rate regimes are distinguished based on the flow rate – frequency response such that a drop in frequency was observed for flow rates beyond the onset of closure/collision.

	L=17 mm	L=22 mm
Onset pressure	0.73 Kpa	0.87 Kpa
Mass flow rate	165 cm^3/s	406 cm^3/s
Phonation frequency	92.9 Hz	88.75Hz

Table 1: Phonation onset data of model larynx.

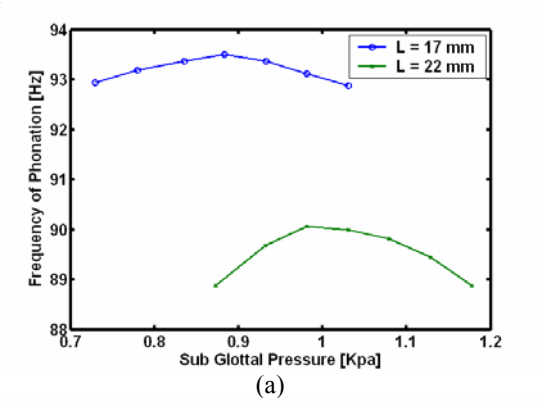

(a)

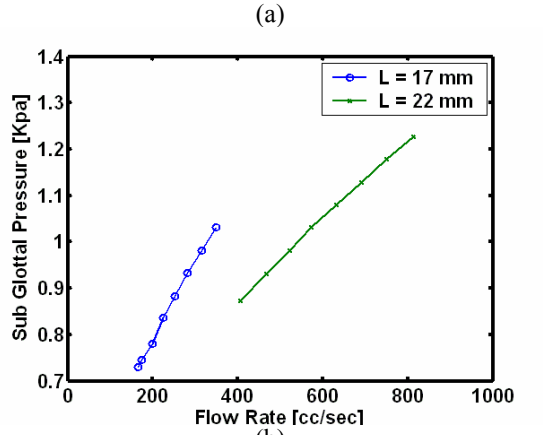

(b)

Figure 4: (a) Phonation frequency vs. Subglottal Pressure; (b) Subglottal pressure vs. mass flow rate for the model with L=17 mm and 22 mm

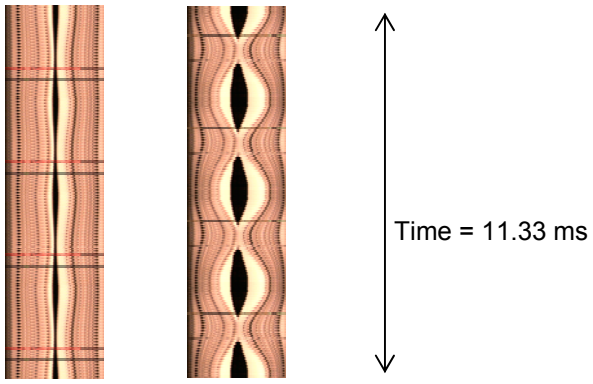

(a) (b)

Figure 5: Sequence of five kymographic images (produced from a single kymographic image) for (a) flow rate of 406 cm^3/s (the phonation threshold), and (b) flow rate of 690 cm^3/s. The Kymographic image location indicated by a line in Figs. 6(a) and (c). L=22 mm.

Figure 6 shows typical digital image analysis results. Superior views of the model larynx are shown for a flow rate of 690 cm^3/s at maximum glottal opening, Fig. 6(a), and during the stage of glottal closure, Fig. 6(c). Figures 6(b) and (d) shows the distribution of the transverse strain component, ε_{xx} obtained from DIC on the superior surface for the images in Fig. 6(a) and (c), respectively. The strain contours are shown on the deformed superior surface. In the position of maximum opening the vocal folds are deformed by a combination of a bulging-type deformation and the opening motion. The maximum value of the out-of-plane displacement was determined to be $w_{\max} = 3.5$ mm. This value is larger than that reported in humans, e.g. in [4] $w_{\max} = 1.5$ mm was reported. At the point of maximum glottal opening, the transverse strain, ε_{xx}, is less than zero at the mid-section of the superior surface. During the closing process vocal fold contact occurs, Fig. 6(c). Closure of the glottal opening is not complete and two distinct open areas are visible during the closing stage. These open areas are located at the anterior and posterior ends of the model larynx; see Fig. 6(c). Such incomplete closure has been observed in actual glottal measurements [15] and 3D finite element simulations [16]. Even during the closing stage the model larynx retains some of the bulging deformation. A local minimum of the out- of-plane displacement is seen at the midsection of the superior surface, $w = 1.65$ mm, while the two locations of maximum out-of-plane displacement, $w = 1.81$ mm, coincide with the locations of partial opening. During closure the characteristics of the strain fields changes significantly. At the midsection of the vocal folds the strain, ε_{xx}, is positive (tensile stress) and significant in amplitude, $\varepsilon_{xx} \approx 0.1$.

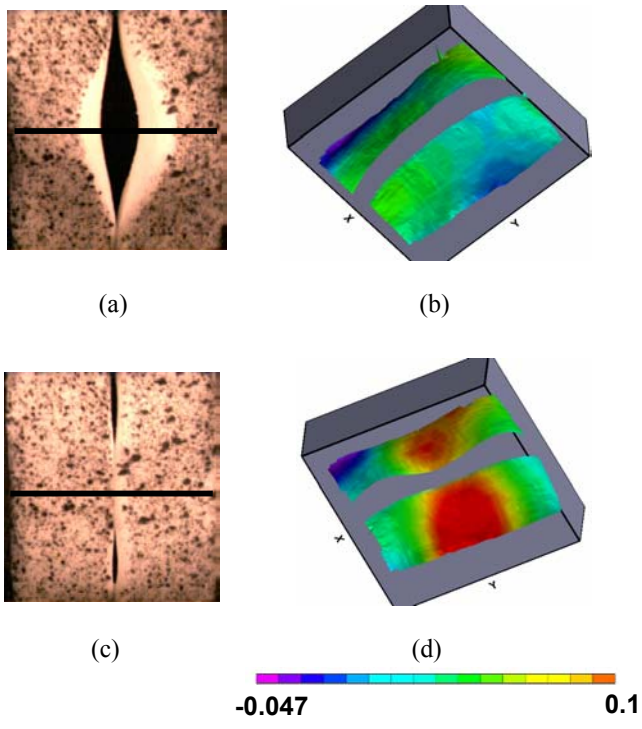

(a) (b)

(c) (d)

Figure 6: The model larynx ($L = 22$ mm, flow rate of 690 cm^3/s) (a) Image at maximum open position; and (b) contour of ε_{xx}; (c) image for closed state; and (d) contour of ε_{xx}.

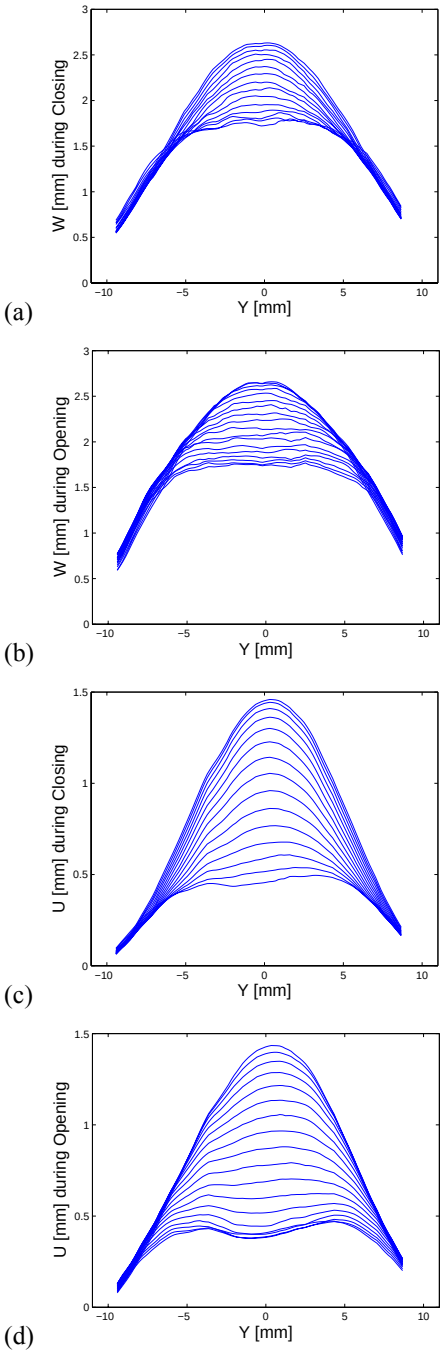

Figure 7: Out-of plane (a, b) and in-plane (c,d) displacements along the medial surface. L=22mm

The DIC method was also used to extract details of the time history of the wall displacement. Figure 7 shows the out-of-plane (w) and in-plane (u) displacements obtained for points along a line parallel to the medial surface at a position 1.5 mm from the centerline of the undeformed larynx for a flow rate of 406 cm^3/s. Fig. 7(a) and (b) show that the model larynx remains in a bulged state due to the mean static pressure in all stages, $w_{\max}$ =2.63 mm and $w_{\min}$ =1.72 mm. The main out-of-plane vibratory displacements occur in the center of the vocal fold over a span of around L/2 with the outer parts of the folds almost fixed during oscillation. The range of the out-of-plane displacement was found to be $\Delta w = 0.91$ mm. Figs. 7(c) and (d) illustrate the process of glottal opening. The model larynx remains in an open state due to the mean static pressure in all stages, $u_{\max}$ =1.45 mm and $u_{\min}$ = 0.40 mm. The main vibratory displacement occurs again in the center section of the vocal fold over a length of 3L/4. The range of the in-plane displacement was $\Delta u = 1.10$ mm.

V. CONCLUSION

The application of a three-dimensional DIC method for the non-contact and non-invasive measurements of displacement and strain fields in self-oscillating vocal folds has been described. The method was implemented and applied in the laboratory to measurements of the superior vocal fold surface of a rubber physical model. It provided time-resolved, full field measurements of several parameters of interest in phonation studies, including the out-of-plane displacements (the so-called mucosal wave height), the glottal opening displacement, as well as the strain fields corresponding to these displacements. The study demonstrates the linear dependence of subglottal pressure over mass flow rate and also the effectiveness of DIC method in estimating the strain fields. Furthermore, it was found that while the out-of-plane displacements exceed those of the in-plane displacements, the vibration amplitudes of these two degrees of freedom are similar. Stress will be obtained from measured mechanical properties of the solid in future studies. The outlook for applications in clinical studies is promising.

ACKNOWLEDGMENTS

This work was supported by grant R01 DC005788 from the National Institute for Deafness and other Communication Disorders (NIH-NIDCD).

REFERENCES

[1] Tigges, M., et al., Proc. SPIE Vol. 2927 (1996) 209-216.
[2] Švec, J. G., et al., J. Acoust. Soc. Am. 108 (2000) pp. 1397.
[3] Berry, D.A., et al., J. Acoust. Soc. Am. 110(2001) pp. 2539.
[4] Manneberg, G., et al., Opt. Eng. 40 (2001) 2041-2044.
[5] Thomson, S. L., Ph.D. Thesis, Purdue University, 2004
[6] Scherer, R.C., et al., J. Acoust. Soc. Am. 109 (2001) pp.1616.
[7] Thomson, S. L., et al. MAVEBA 2003.
[8] Smooth-On, Inc.
[9] Zhang, K., et al., J. Acoust. Soc. Am. (2005) submitted.
[10] NAC Image Technology, Inc.
[11] Chu, C.T., et al., Exp. Mech. 25 (1985) pp. 232.
[12] Helm, J.D., Opt. Eng. 36 (1997) pp. 2361.
[13] Correlated Solutions, Inc.
[14] Sutton P., et al., Image Vision Comp. 4 (1986) pp. 143.
[15] Holzrichter, J.F., et al. J. Acoust. Soc. Am. 117 (2005) pp. 1373.
[16] de Oliveira Rosa, M., et al. J. Acoust. Soc. Am. 114 (2003) pp. 2893.